Phase Diagrams of Earth-Forming Minerals

Dean C. Presnall

The purpose of this compilation is to present a selected and compact set of phase diagrams for the major Earth-forming minerals and to show the present state of knowledge concerning the effect of pressure on the individual mineral stabilities and their high-pressure transformation products. The phase diagrams are arranged as follows:

	Figure
Silica	1
Feldspars	2-7
Pyroxenes	8-13
Olivine	14-16
Garnet	17-20
Iron-titanium oxides	21-23
Pargasite	24
Serpentine	25
Phlogopite	25
Iron	26-27

The compilation has been compressed in three ways. (1) For several of the mineral groups, only representative phase diagrams are shown. (2) The presentation of more complex phase diagrams that show mutual stability relationships among the various minerals and mineral groups has been minimized. (3) Many subsolidus phase diagrams important to metamorphic petrology and thermobarometry are excluded. Reviews of these subsolidus phase relationships and thermodynamic data for calculating the phase diagrams have been presented elsewhere [13, 50, 70, 122, 154]. Other useful reviews and compilations of phase diagrams are Lindsley [96] for oxides, Gilbert *et al.* [60] and Huckenholz *et al.* [74] for amphiboles, Liu and Bassett [104] for elements, oxides, and silicates at high pressures, and *Phase Diagrams for Ceramists* [129-137]. It will be noted that some diagrams are in weight percent and others are in mole percent; they have usually been left as originally published. Minor drafting errors and topological imperfections that were found on a few of the original diagrams have been corrected in the redrafted diagrams shown here.

D. C. Presnall, University of Texas, Dallas, Geoscience Program, POB 830688, Richardson, TX 75083-0688

Mineral Physics and Crystallography
A Handbook of Physical Constants
AGU Reference Shelf 2

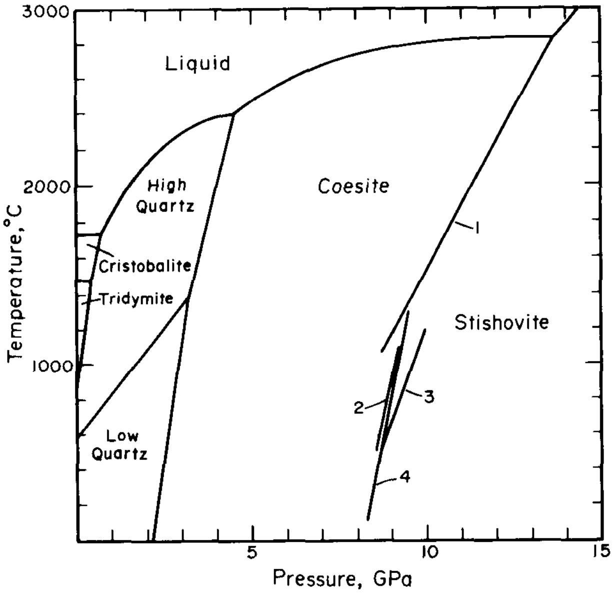

Fig. 1. Phase relationships for SiO_2. Numbers beside curves refer to the following sources: 1 - [178]; 2 - [168]; 3 - [160]; 4 - [4]. The melting curve is from Jackson [77] at pressures below 4 GPa, from Kanzaki [83] at pressures between 4 and 7 GPa, and from Zhang *et al.* [178] at pressures above 7 GPa. The temperature of the high quartz-low quartz-coesite invariant point is from Mirwald and Massonne [113]. The quartz-coesite transition is from Bohlen and Boettcher [24] but note that their curve lies toward the low-pressure side of the range of curves by others [5, 23, 31, 62, 89, 113]. The high quartz-low quartz curve is from Yoder [172]. Boundaries for the tridymite and cristobalite fields are from Tuttle and Bowen [164] except that the cristobalite-high quartz-liquid invariant point has been shifted to 0.7 GPa to accomodate the data of Jackson [77]. Silica has been synthesized in the Fe_2N structure at 35-40 GPa, T>1000°C by Liu *et al.* [105], and at 35 GPa, 500-1000°C by Togaya [162]. However, Tsuchida and Yagi [163] reported a reversible transition between stishovite and the $CaCl_2$ structure at 80-100 GPa and T>1000°C.

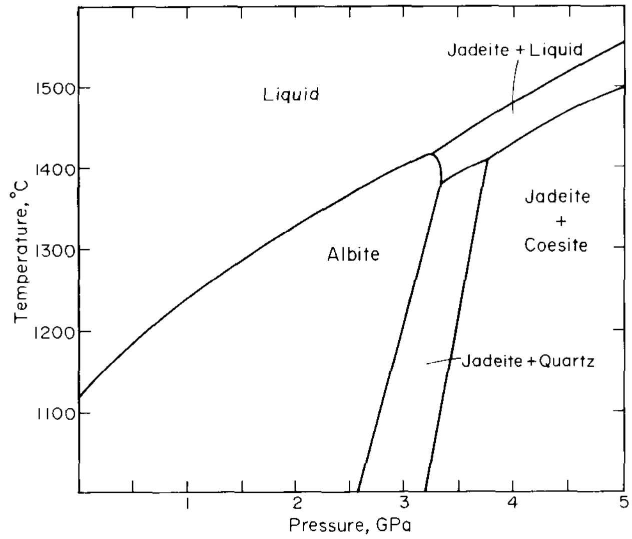

Fig. 2. Isopleth for the composition, $NaAlSi_3O_8$ [12, 16, 33]. The albite = jadeite + quartz reaction shown by Bell and Roseboom [12] and in this figure is about 0.1 GPa higher than the curve of Boettcher and Wyllie [22]. The latter passes through the "consensus" value of 1.63 GPa, 600°C for this reaction [81]. Also, the quartz-coesite curve shown by Bell and Roseboom [12] and in this figure is about 0.4 GPa higher at 1300°C than the pressure given by a linear extrapolation of the curve of Bohlen and Boettcher [24], which is shown in Figure 1. The curve of Bohlen and Boettcher would intersect the albite = jadeite + quartz curve at about 1300°C rather than the jadeite + quartz (coesite) = liquid curve. At about 1000°C, Liu [101] synthesized $NaAlSi_3O_8$ in the hollandite structure at pressures from 21 to 24 GPa, and a mixture of $NaAlSiO_4$ ($CaFe_2O_4$-type structure) + stishovite above 24 GPa. Jadeite, $NaAlSi_2O_6$; Coesite, SiO_2.

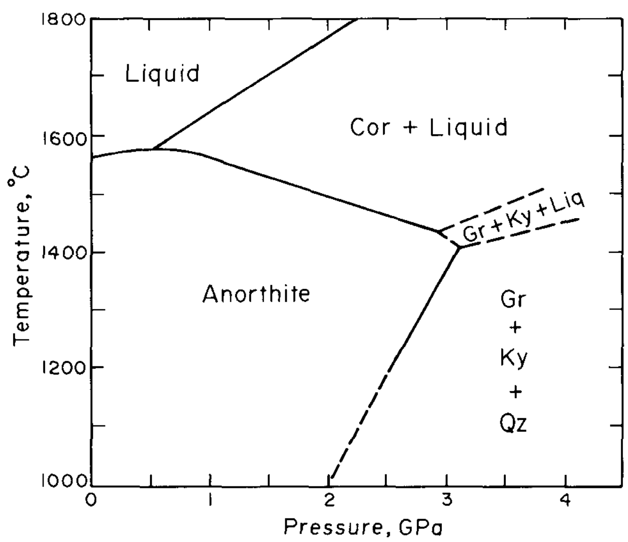

Fig. 3. Isopleth for the composition, $CaAl_2Si_2O_8$ [67, 94]. Cor, corundum; Gr, grossular; Ky, kyanite; Qz, quartz; Liq, liquid. Locations of dashed lines are inferred.

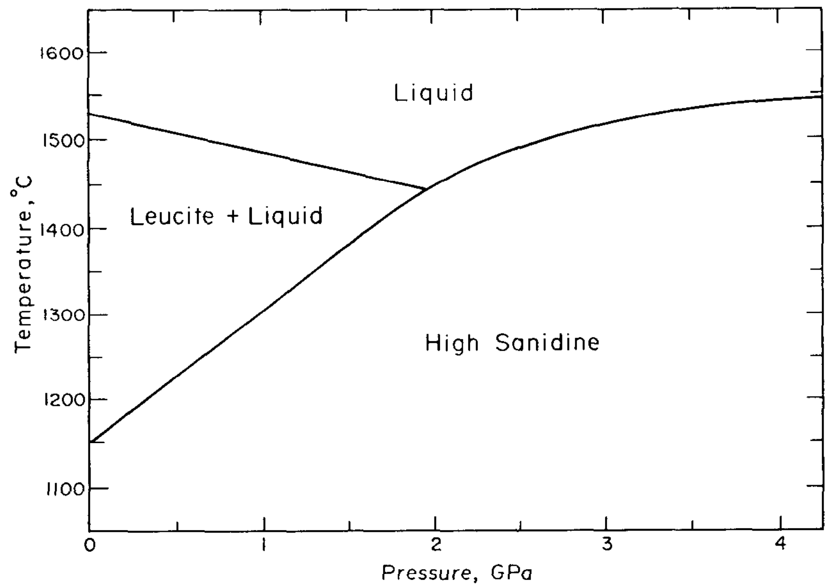

Fig. 4. Isopleth for the composition, $KAlSi_3O_8$ [93, 149]. At 12 GPa, 900°C, Ringwood *et al.* [144] synthesized $KAlSi_3O_8$ in the hollandite structure. In experiments from 8-10 GPa and 700°-1000°C, Kinomura *et al.* [88] synthesized the assemblage $K_2Si_4O_9$ (wadeite-type structure) + kyanite (Al_2SiO_5) + coesite (SiO_2) from the composition $KAlSi_3O_8$; and they synthesized the hollandite structure of $KAlSi_3O_8$ at 900°C, 12 GPa, and at 700°C, 11 and 11.5 GPa.

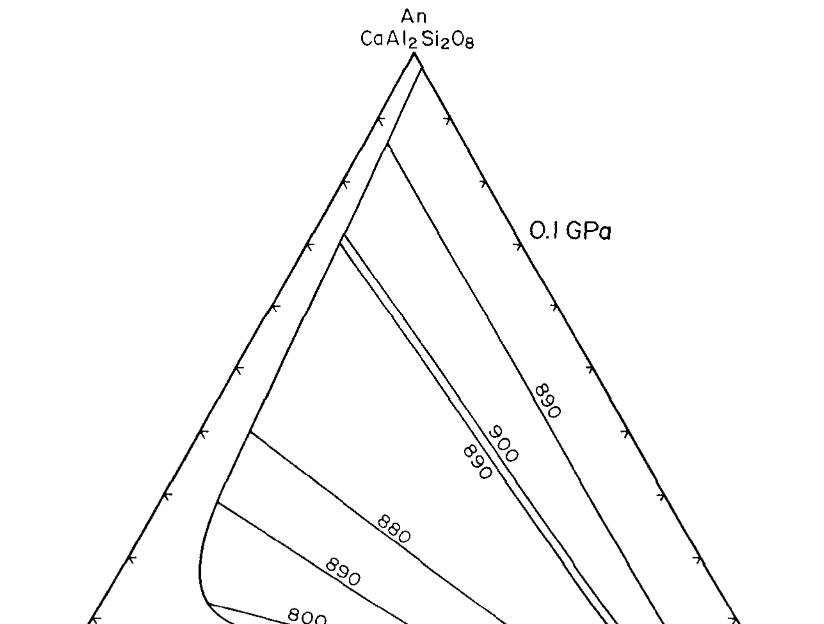

Fig. 5. Compositions of coexisting alkali feldspar and plagioclase at 0.1 GPa and temperatures from 800 to 900°C, as indicated [49]. Note that the phase boundary is essentially isothermal except in the Ab-rich portion of the diagram. Many others have discussed ternary feldspar geothermometry [10, 39, 54, 58, 63, 66, 75, 80, 139, 142, 151-153, 165] and ternary feldspar phase relationships [68, 121, 156, 164, 175]. An, anorthite; Ab, albite; Or, orthoclase.

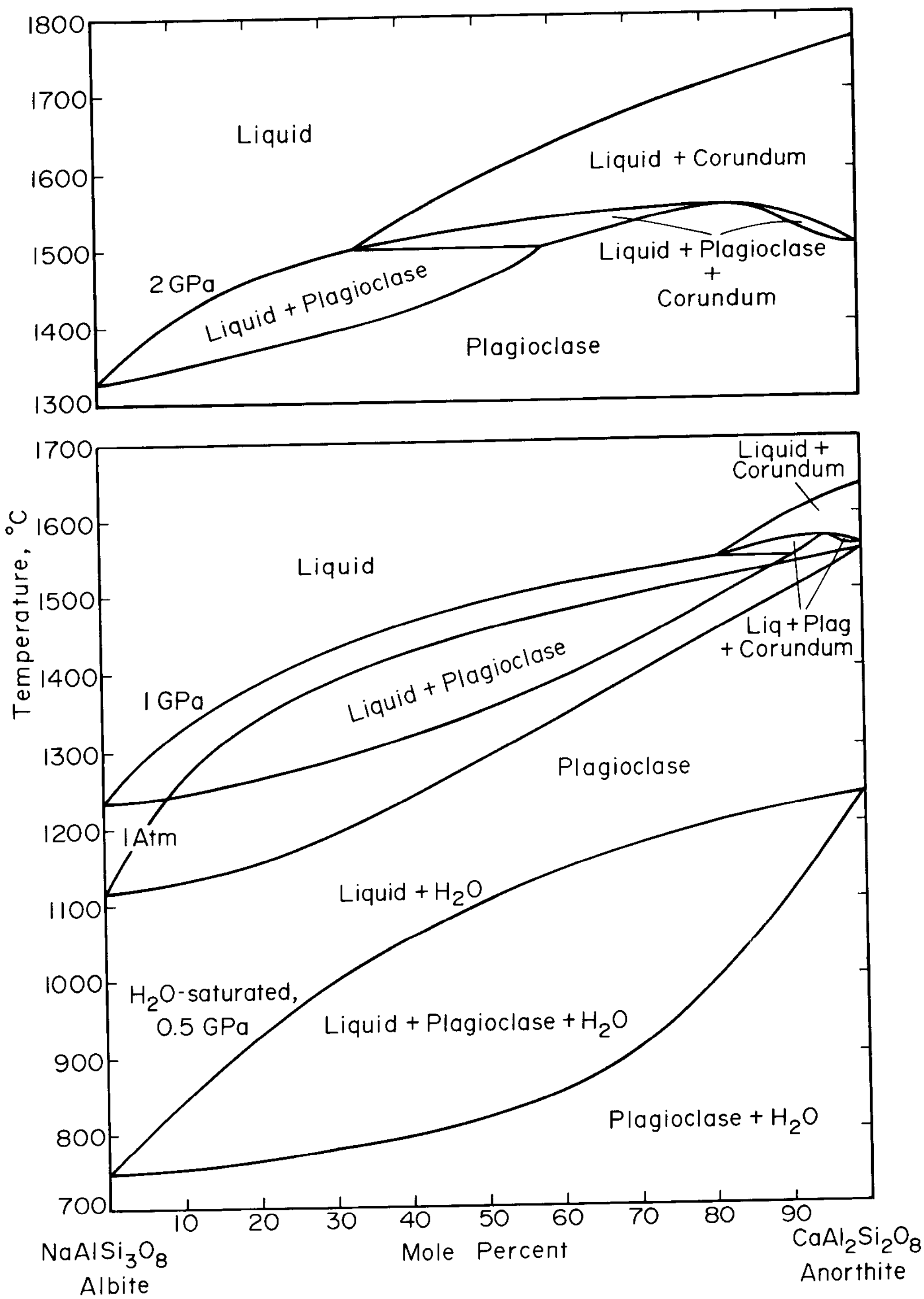

Fig. 6. Temperature-composition sections for the join $NaAlSi_3O_8$ (albite) - $CaAl_2Si_2O_8$ (anorthite) under anhydrous conditions at 1 atm [26, 117], 1 GPa, 2 GPa [33, 94], and under H_2O-saturated conditions at 0.5 GPa [79, 175].

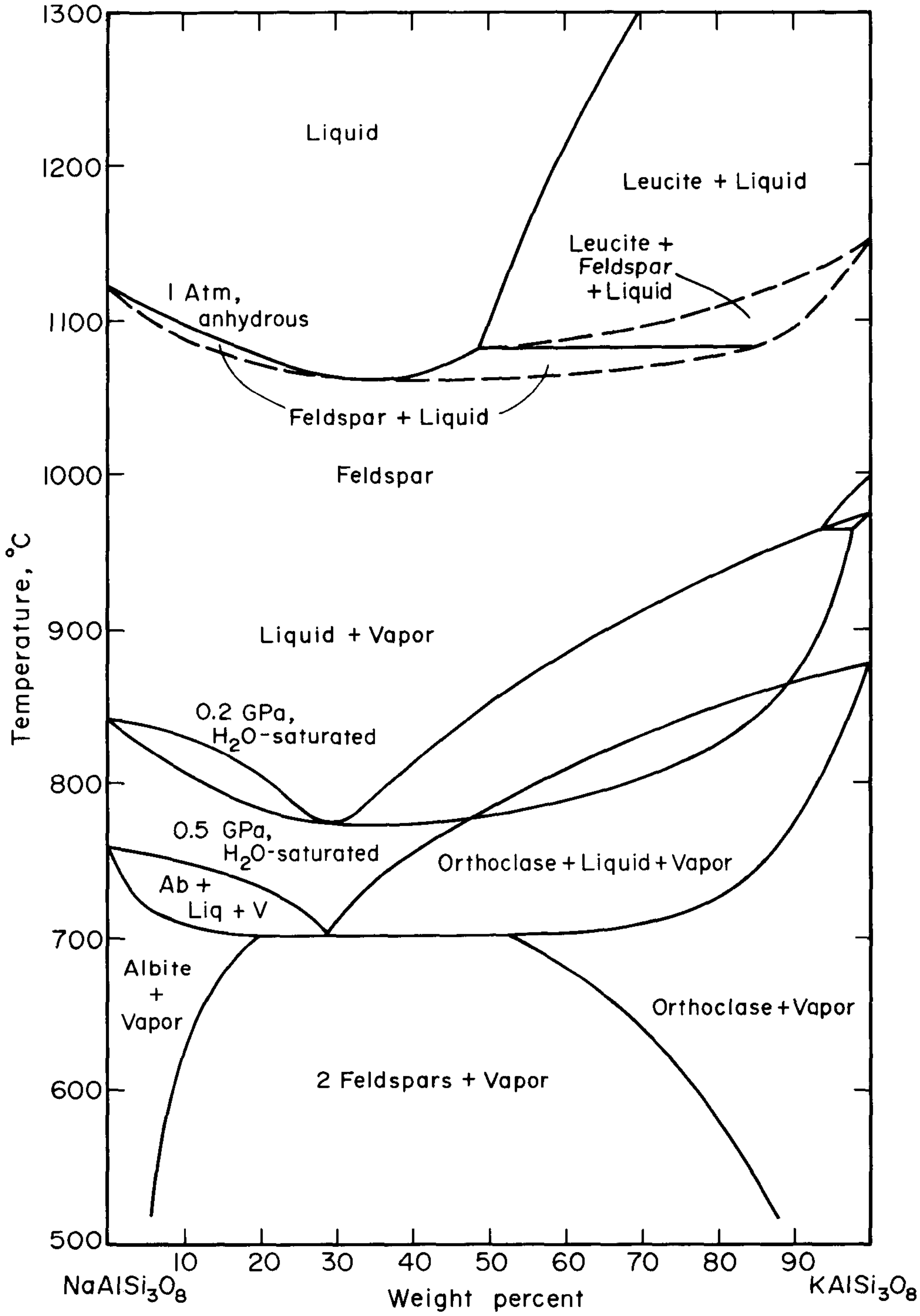

Fig. 7. Temperature-composition sections for the join $NaAlSi_3O_8$ (albite) - $KAlSi_3O_8$ (orthoclase) under anhydrous conditions at 1 atm [148], and under H_2O-saturated conditions at 0.2 GPa [29] and 0.5 GPa [119, 175]. Ab, albite; Liq, liquid; V, vapor. Locations of dashed lines are inferred.

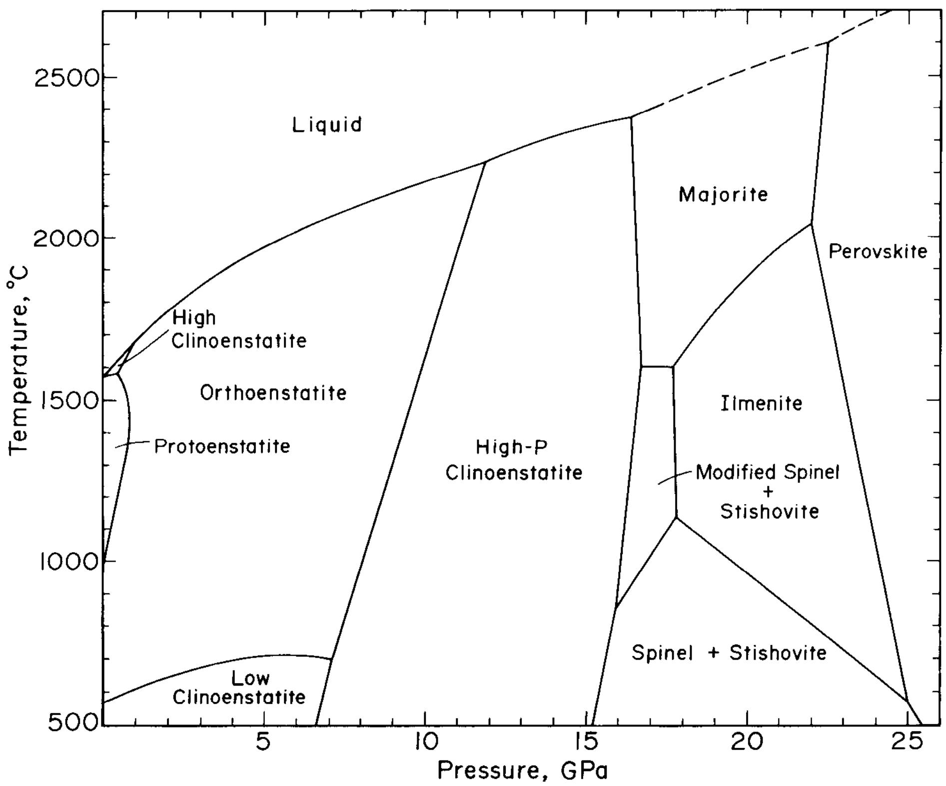

Fig. 8. Isopleth for the composition $MgSiO_3$ [7, 9, 35, 45, 56, 57, 65, 76, 92, 127, 140, 169]. For additional data at pressures above 15 GPa, see also Sawamoto [147]. Not shown is a singular point at about 0.13 GPa below which enstatite melts incongruently to forsterite + liquid [45]. Position of dashed curve is inferred. For additional data on melting temperatures up to 58 GPa, see Zerr and Boehler [177].

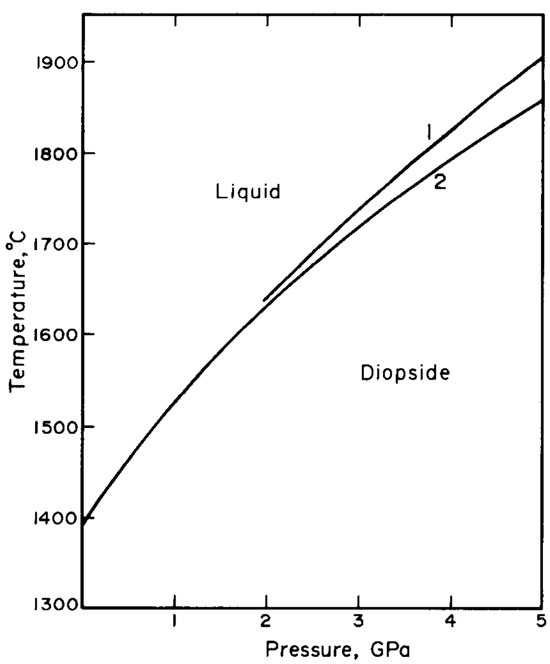

Fig. 9. Melting curve for diopside, $CaMgSi_2O_6$. Curve 1 is from Williams and Kennedy [166] uncorrected for the effect of pressure on thermocouple emf, and curve 2 is from Boyd and England [33]. See also Yoder [173] for data below 0.5 GPa. For $CaMgSi_2O_6$ composition, Mao *et al.* [110] found a mixture of perovskite ($MgSiO_3$) and glass at 21.7 and 42.1 GPa and 1000°-1200°C. They interpreted the glass to be a second perovskite phase of $CaSiO_3$ composition which inverted to glass on quenching [see also 102].

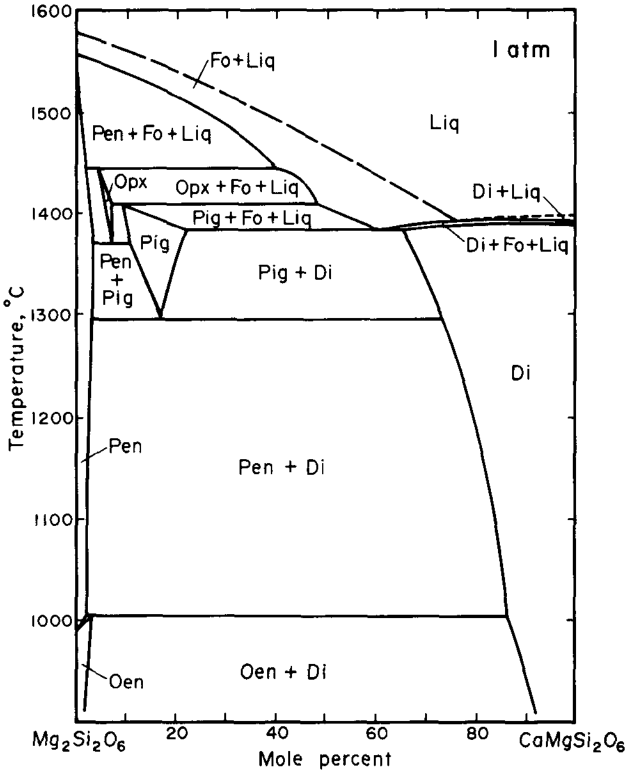

Fig. 10. The join $Mg_2Si_2O_6$ (enstatite) - $CaMgSi_2O_6$ (diopside) at 1 atm [43]. Many others have also discussed phase relationships on this join [9, 14, 36, 41, 42, 56, 78, 91, 106, 170, 171]. Fo, forsterite, Mg_2SiO_4; Liq, liquid; Pen, protoenstatite; Opx, orthopyroxene; Pig, pigeonite; Di, diopside; Oen, orthoenstatite.

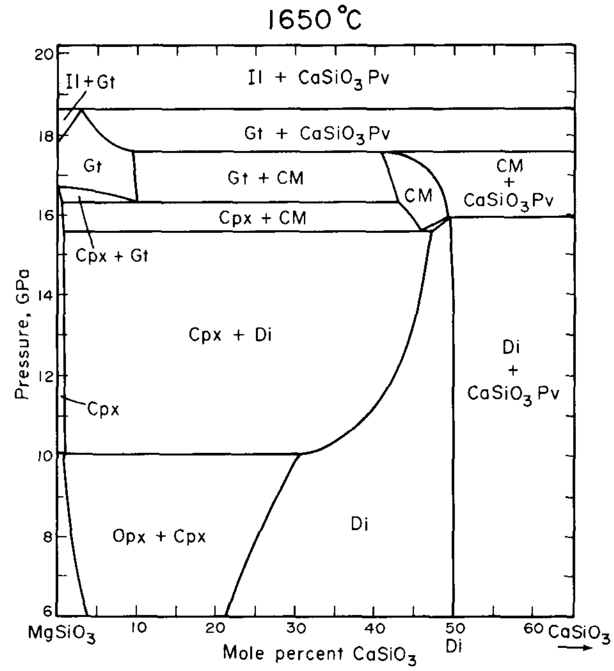

Fig. 12. Pressure-composition section for the system $MgSiO_3$-$CaSiO_3$ at 1650°C [55, 57]. Garnet and clinopyroxene, when they are free of Ca on the left-hand margin of this diagram, are the same phases, respectively, as majorite and high-P clinoenstatite on Figure 7. Il, ilmenite; Gt, garnet; Pv, perovskite; Cpx, clinopyroxene; Opx, orthopyroxene; Di, diopside; CM, a high-pressure phase of unknown structure.

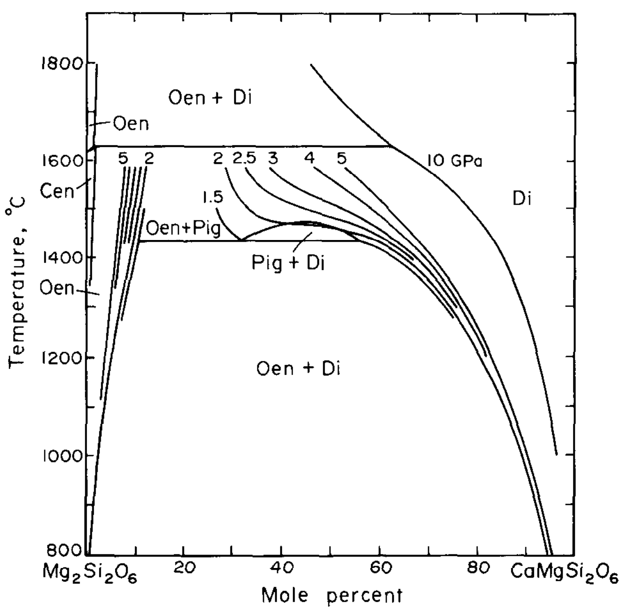

Fig. 11. Thermodynamically modeled subsolidus phase relationships for the system $Mg_2Si_2O_6$ (enstatite) - $CaMgSi_2O_6$ (diopside) from 1.5 to 10 GPa [56, 44]. The thermodynamic models are based on data from other sources [37, 98, 118, 123, 128, 150]. See also data of Biggar [15] from 1 atm to 0.95 GPa.

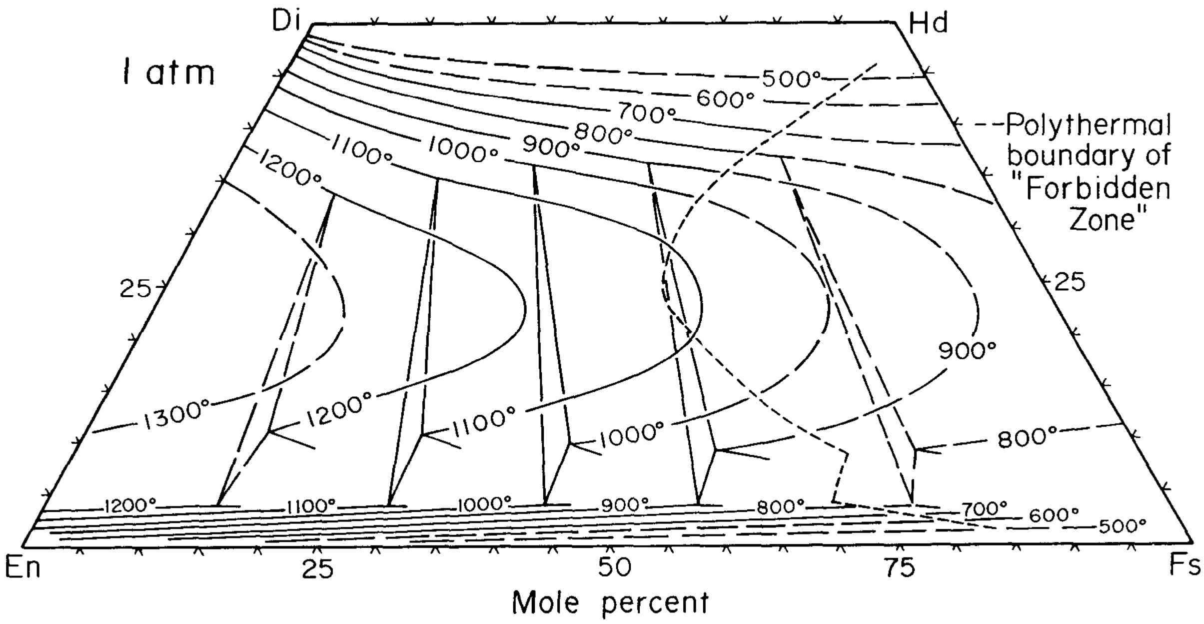

Fig. 13. Orthopyroxene + augite, orthopyroxene + augite + pigeonite, and pigeonite + augite equilibria at 1 atm and 500-1300°C [95]. Phase relationships to the right of the forbidden zone boundary are metastable relative to augite + olivine + silica. Lindsley [95] has presented three other similar diagrams at 0.5, 1, and 1.5 GPa. Lindsley and Andersen [97] should be consulted for correction procedures required before plotting pyroxenes on these diagrams for geothermometry. En, enstatite ($MgSiO_3$); Fs, ferrosilite ($FeSiO_3$); Di, diopside ($CaMgSi_2O_6$); Hd, hedenbergite ($CaFeSi_2O_6$).

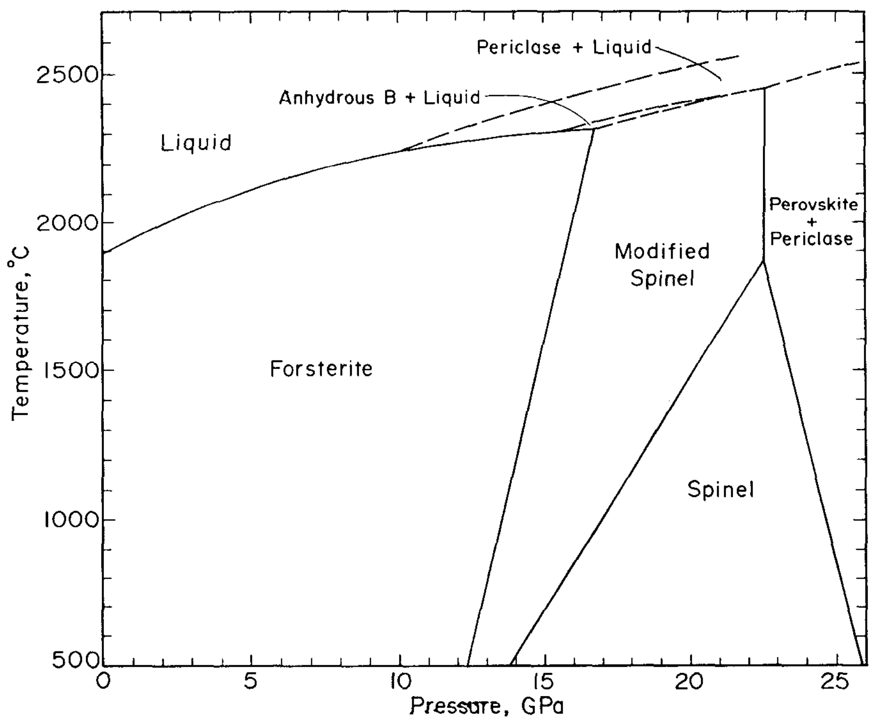

Fig. 14. Isopleth for the composition Mg_2SiO_4 [48, 57, 141]. Additional studies of the melting relationships are Ohtani and Kumazawa [126] and Kato and Kumazawa [84-86]. Locations of dashed lines are inferred.

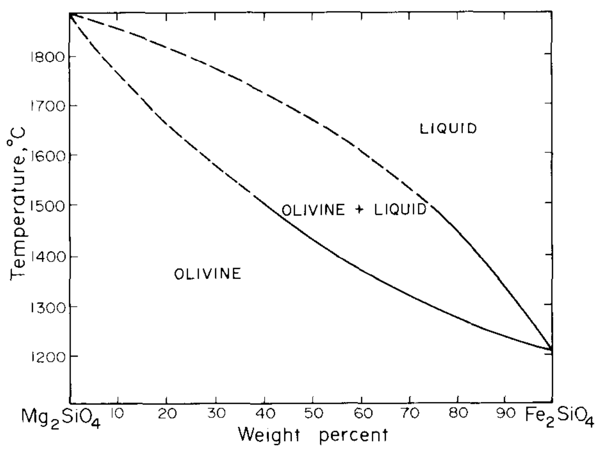

Fig. 15. Phase relationships for the system Mg_2SiO_4 (forsterite) - Fe_2SiO_4 (fayalite) in equilibrium with Fe at 1 atm [27]. Locations of dashed lines are inferred.

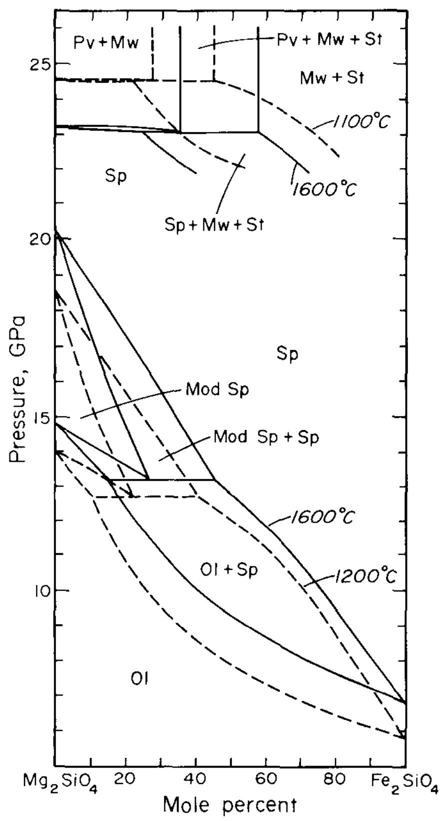

Fig. 16. Pressure-composition sections for the join Mg_2SiO_4-Fe_2SiO_4 at various temperatures. Phase relationships above 21 GPa are from Ito and Takahashi [76] and those below 21 GPa are from Akaogi *et al.* [3]. Other references [51, 87, 157] give additional data and discussion of these phase relationships. Pv, perovskite ($MgSiO_3$-$FeSiO_3$ solid solution); Mw, magnesiowüstite (MgO-FeO solid solution); St, stishovite (SiO_2); Sp, spinel; Mod Sp, modified spinel; Ol, olivine.

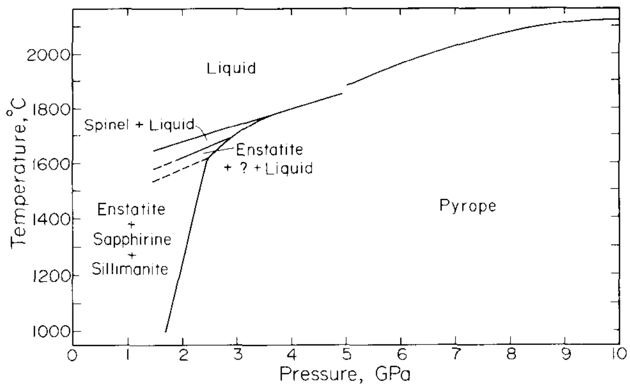

Fig. 17. Isopleth for $Mg_3Al_2Si_3O_{12}$, pyrope garnet. Phase relationships at pressures less than 5 GPa are from Boyd and England [32]. The melting curve at 5 GPa and above is from Ohtani *et al.* [125]. Liu [99] reported that pyrope transforms to perovskite + corundum at about 30 GPa, 200-800°C. Liu [100] subsequently revised this result and found that pyrope transforms to the ilmenite structure at about 24-25 GPa, 1000°-1400°C, and that ilmenite then transforms to perovskite at about 30 GPa. Locations of dashed lines are inferred.

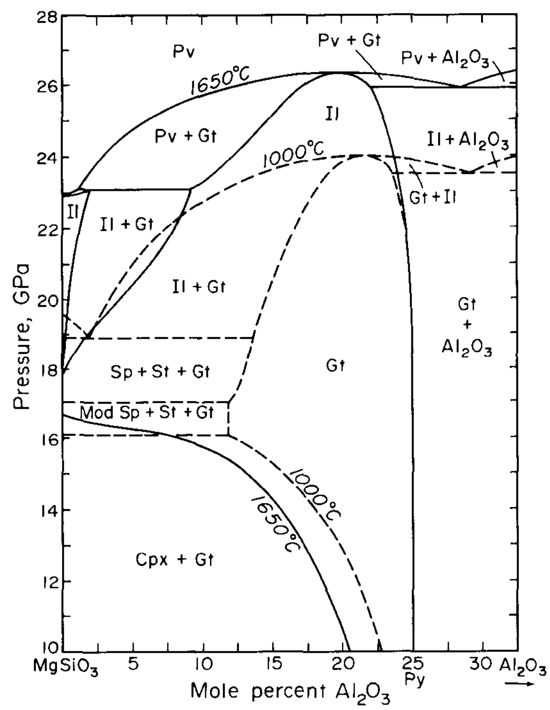

Fig. 18. Pressure-composition section for the join $MgSiO_3$-Al_2O_3 at 1000 and 1650°C [57, 82]. For additional data along the boundary between the garnet and clinopyroxene + garnet fields at 1000°C, see Akaogi and Akimoto [2]. At 1100 and 1600°C for pressures between 2 and 6.5 GPa, the Al_2O_3 content of pyroxene in equilibrium with garnet increases with decreasing pressure to at least 15 mole percent [30, 34].

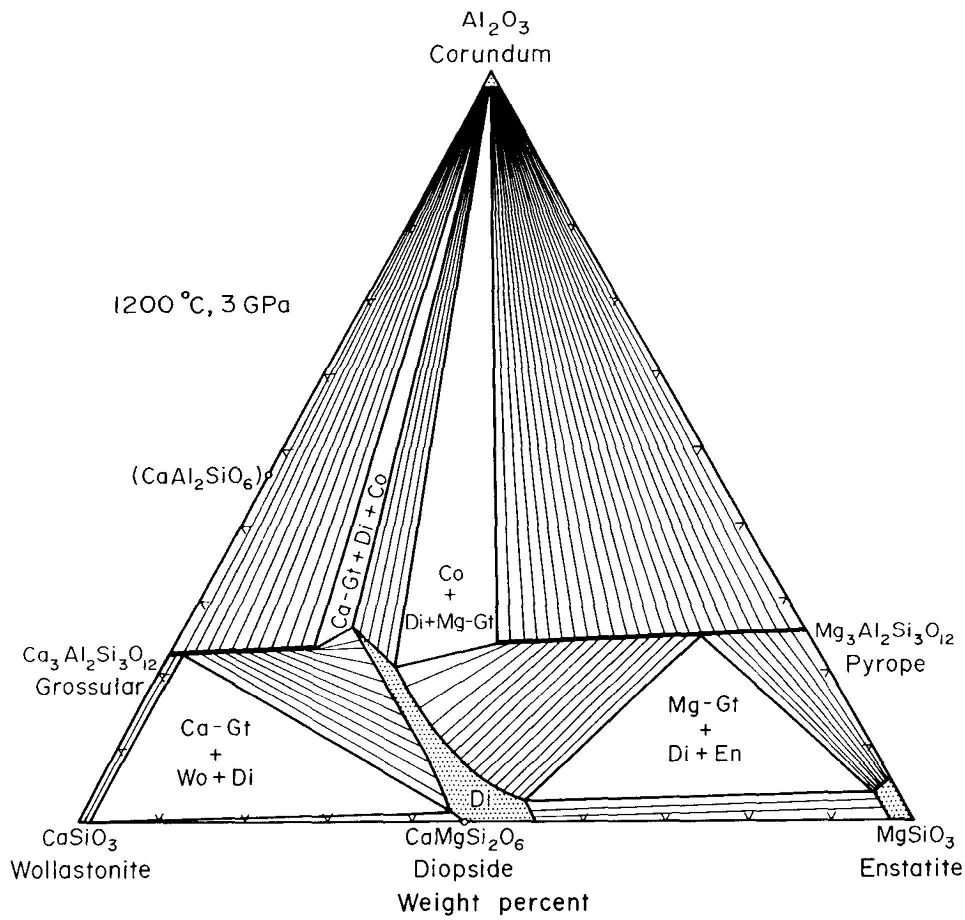

Fig. 19. The system $CaSiO_3$-$MgSiO_3$-Al_2O_3 at 1200°C, 3 GPa [30]. Co, corundum; Di, diopside; Ca-Gt, Ca-garnet; Mg-Gt, Mg-garnet; Wo, wollastonite; En, enstatite; $CaAl_2SiO_6$, Ca-Tschermak's molecule.

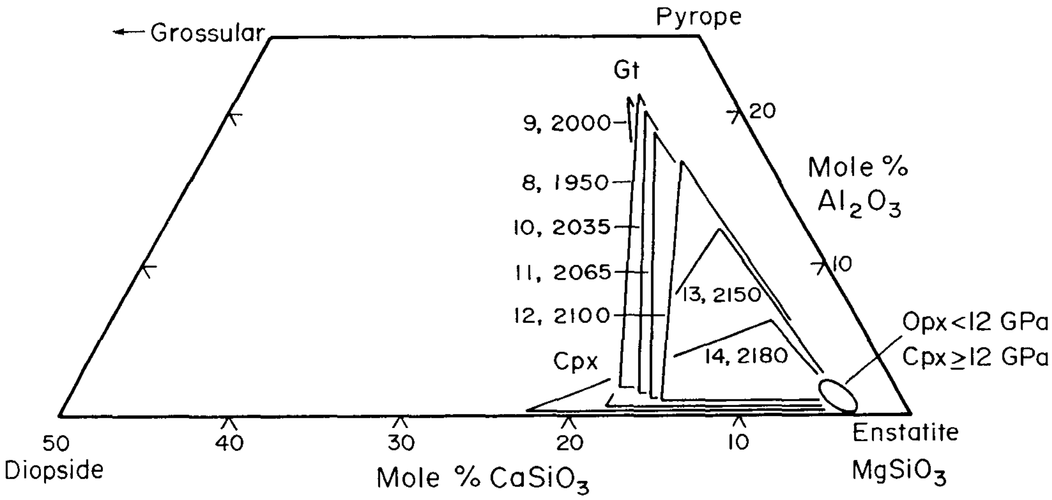

Fig. 20. Compositions (unsmoothed) of coexisting garnet (Gt), Ca-rich pyroxene (Cpx), and Ca-poor pyroxene (Opx or Cpx) at various pressures and temperatures [69]. Labels of the type, 9, 2000, indicate pressure (GPa) followed by temperature (°C). Pyrope, $Mg_3Al_2Si_3O_{12}$; Grossular, $Ca_3Al_2Si_3O_{12}$.

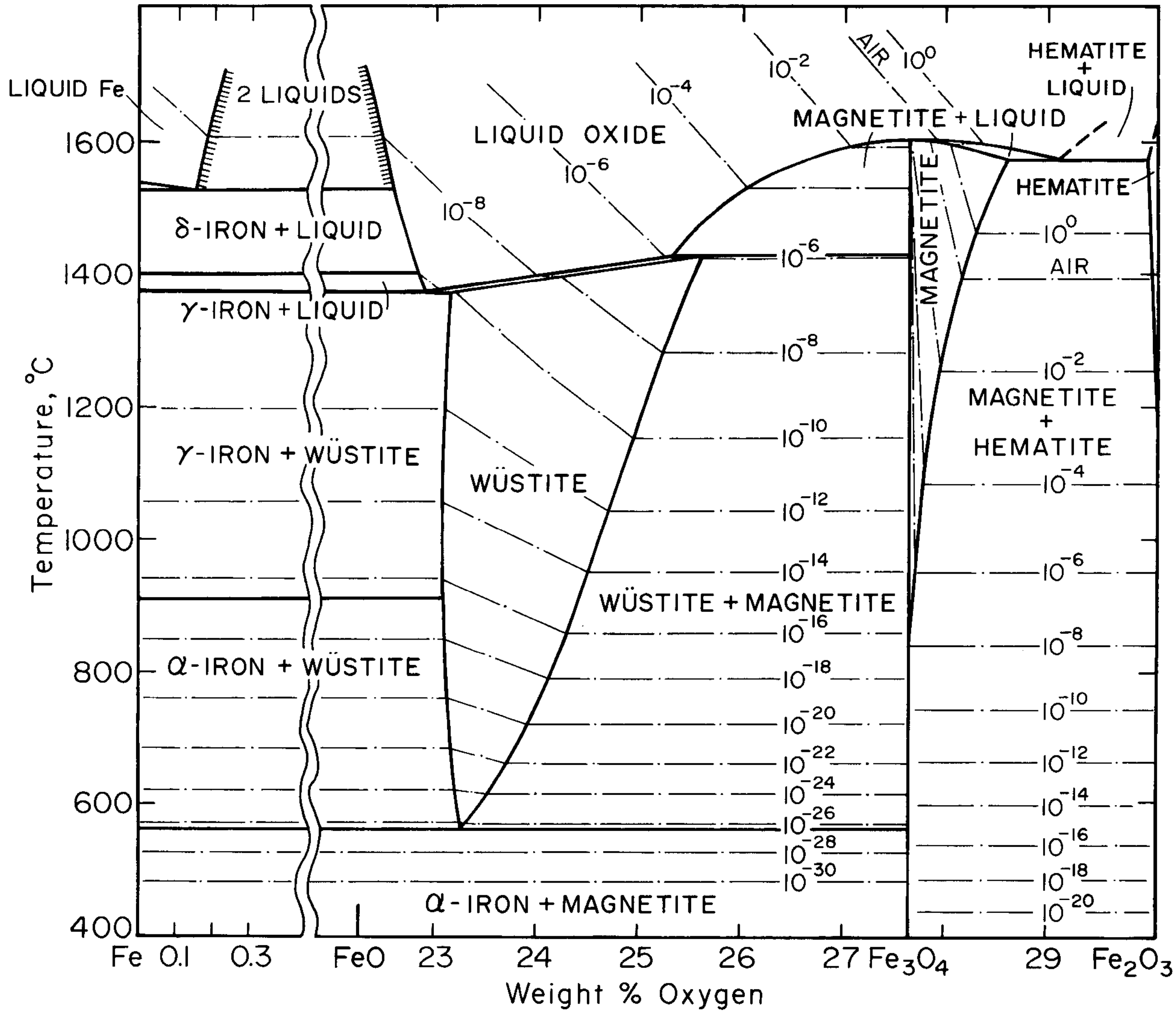

Fig. 21. Temperature-composition section for the system Fe-O at 1 atm [46, 47, 64, 120, 138]. Light dash-dot lines are oxygen isobars in atm.

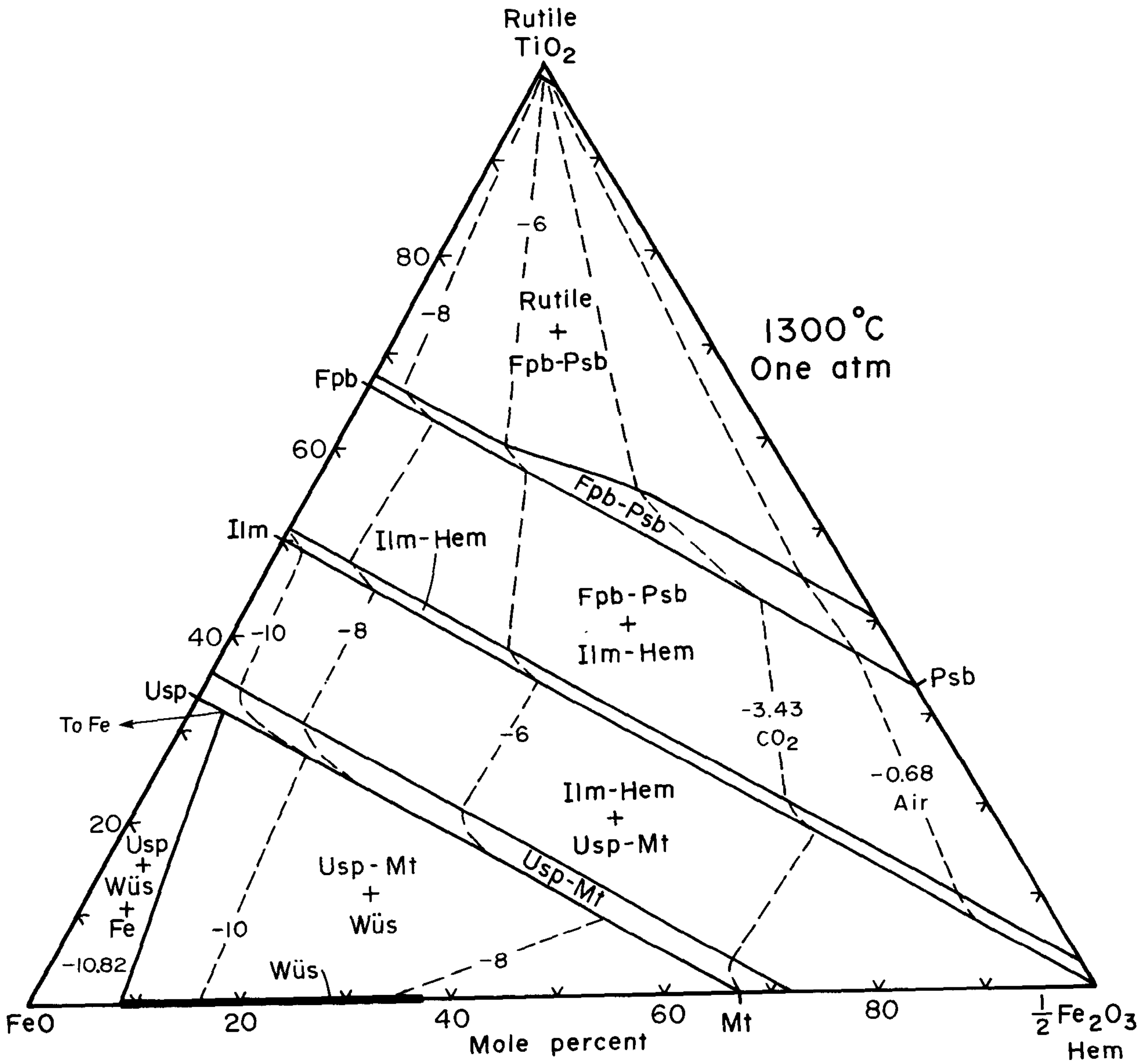

Fig. 22. The system TiO_2-FeO-Fe_2O_3 at 1300°C, 1 atm [161]. Light dashed lines are oxygen isobars labeled in log oxygen fugacity units (atm). Psb, pseudobrookite (Fe_2TiO_5); Fpb, ferropseudobrookite ($FeTi_2O_5$); Ilm, ilmenite ($FeTiO_3$); Hem, hematite (Fe_2O_3); Usp, ulvospinel (Fe_2TiO_4); Mt, magnetite (Fe_3O_4); Wüs, wüstite ($Fe_{1-x}O$).

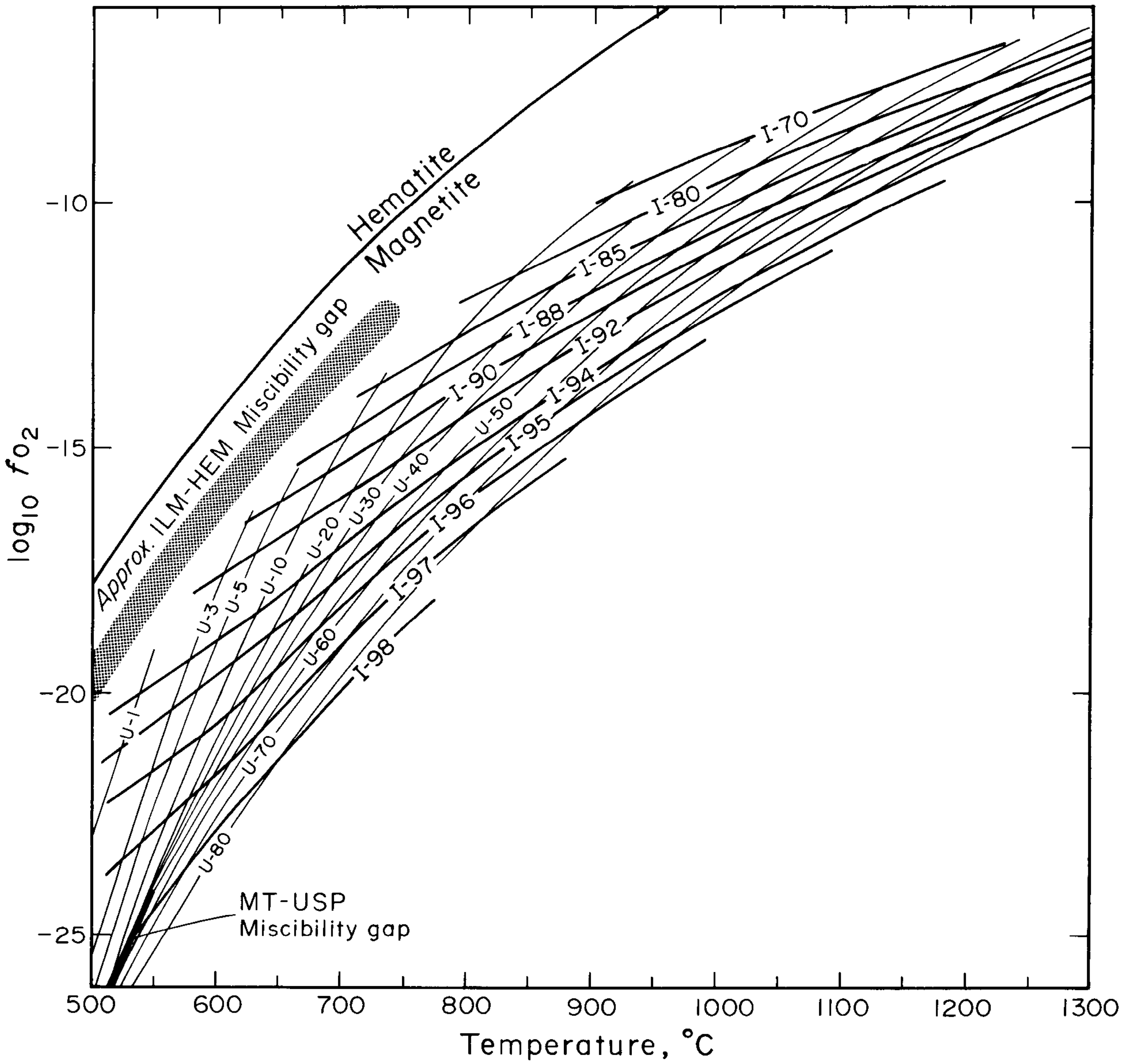

Fig. 23. Temperature-oxygen fugacity (f_{O_2}) grid for coexisting magnetite-ulvospinel solid solution and ilmenite-hematite solid solution pairs [155]. Lines with labels of the type, I-70, indicate mole % ilmenite in the ilmenite ($FeTiO_3$) - hematite (Fe_2O_3) solid solution. Lines with labels of the type, U-70, indicate mole % ulvospinel in the ulvospinel (Fe_2TiO_4) - magnetite (Fe_3O_4) solid solution. Mt, magnetite; Usp, ulvospinel; Ilm, ilmenite; Hem, hematite.

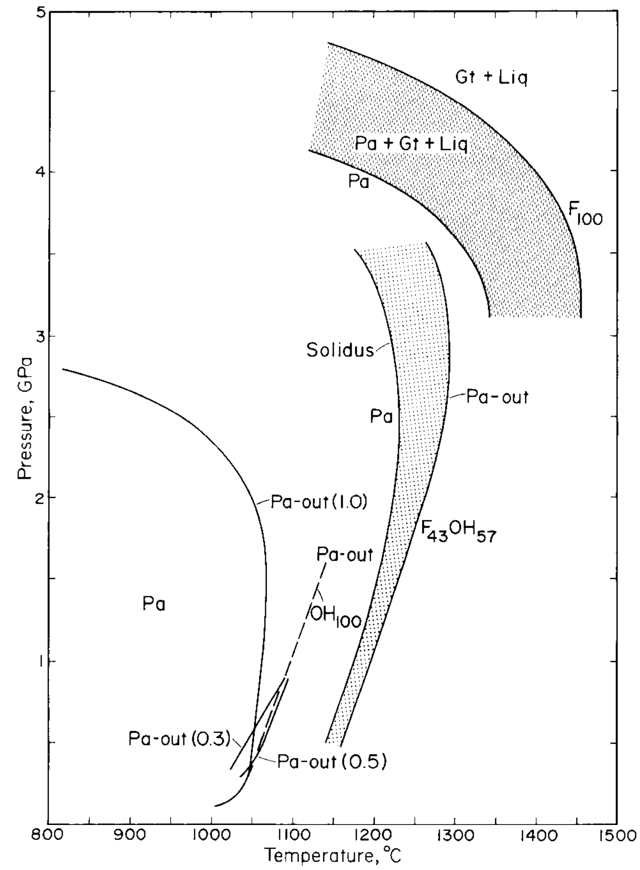

Fig. 24. Pressure-temperature projection of pargasite, (Pa) $NaCa_2Mg_4Al_3Si_6O_{22}(OH,F)_2$, stability limits. The univariant curves labeled Pa-out (1.0), Pa-out (0.5), and Pa-out (0.3) are from Gilbert [59], Holloway [71], and Oba [124], and give the maximum stability of pargasite during melting in the presence of a pure H_2O or H_2O-CO_2 vapor with H_2O mole fractions of 1.0, 0.5, and 0.3. Small concentrations of other constituents in the vapor are ignored. The dashed curve labeled OH_{100}, and the patterned areas labeled $F_{43}OH_{57}$ and F_{100} are from Holloway and Ford [72] and Foley [52], and show the breakdown of pargasite during vapor-absent melting for different proportions of fluorine and hydroxyl in the pargasite.

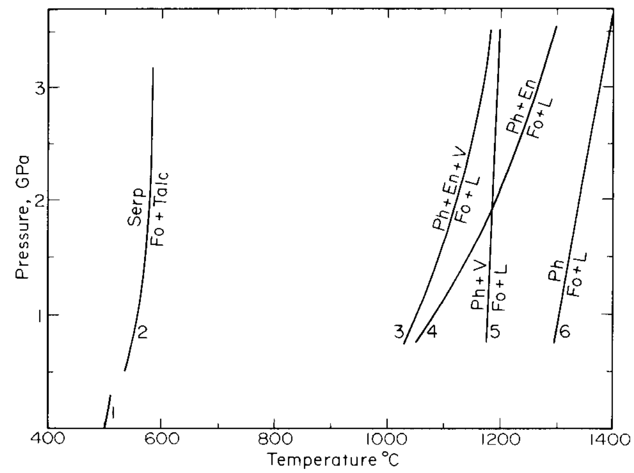

Fig. 25. Pressure-temperature projection showing the upper temperature stability limits for serpentine, $Mg_3Si_2O_5(OH)_4$ (curves 1 and 2), and phlogopite, $KMg_3AlSi_3O_{10}(OH)_2$ (curves 3-6). Numbers beside curves refer to the following sources: 1 - [28]; 2 - [90]; 3-6 - [115]. Curves 5 and 6 give the maximum stability of phlogopite in the presence (curve 5) and absence (curve 6) of vapor. Curves 3 and 4 give the corresponding maximum stability of phlogopite in the presence of forsterite and enstatite, and represent more closely the stability of phlogopite in the mantle. Curves 3-6 are not univariant [114]. See Yoder and Kushiro [174] for an earlier study of the stability of phlogopite. Montana and Brearley [116] speculated that a singular point exists at about 1.5 GPa on curve 4, so that the curve above this pressure is metastable.

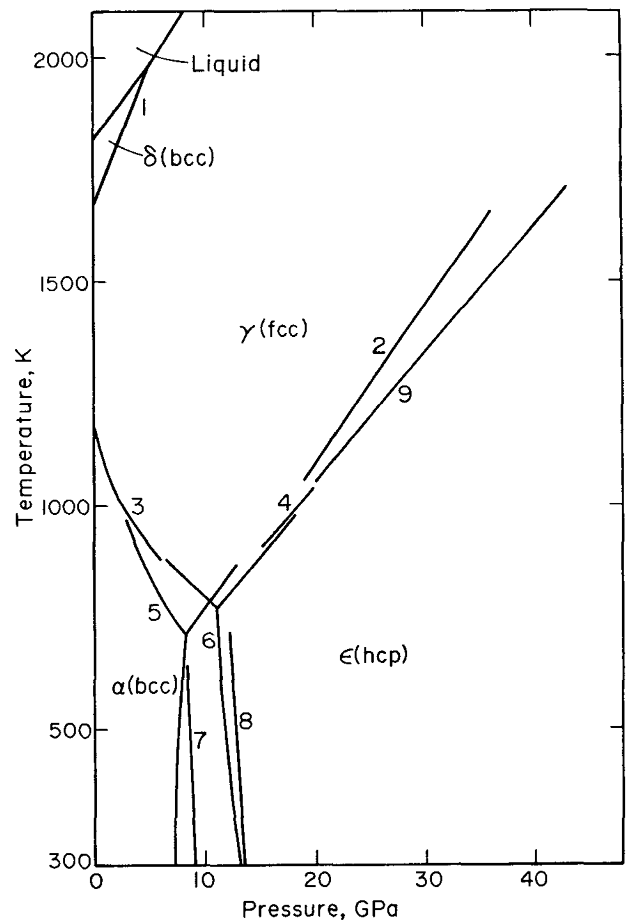

Fig. 26. Low pressure phase relationships for iron. Numbers beside curves refer to the following sources: 1 - [159]; 2 - [109]; 3 - [112]; 4 - [103]; 5 - [6]; 6 - [20, 40]; 7 - [107]; 8 - [73]; 9 - [17, 21]. Several additional references [61, 108, 179] also discuss the α-ε transition,.

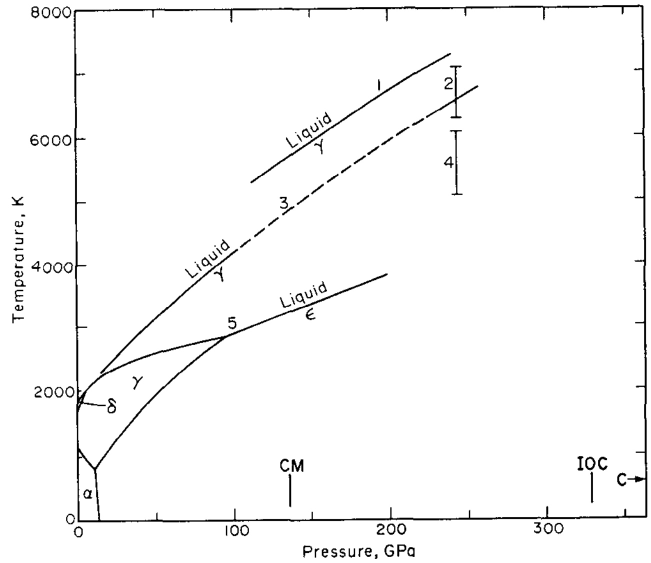

Fig. 27. High pressure melting curves for iron. For reference to Figure 26 at low pressures, the curves of Mirwald and Kennedy [112], Bundy [40], and Boehler [17] are used for the α-ε-γ phase relationships. Numbers beside melting curves and brackets refer to the following sources: 1 - [1]; 2 - [11]; 3 - [167]; 4 - [25, 38]; 5 - [17-19, 21, 103, 143, 153]. Gallagher and Ahrens [54] found that earlier shock data from their laboratory [11] are 1000°K too high, which brings the data of Bass *et al.* [11] and Brown and McQueen [38] into agreement. The shock data of Yoo *et al.* [176] (not plotted but located at 6350 K, 235 GPa and 6720 K, 300 GPa) are at slightly higher temperatures than the data of Brown and McQueen. (Ross *et al.* [145] and Anderson [8] have proposed the existence of a new phase, α'-iron, that is stable along the liquidus at pressures above about 170 GPa. On the basis of molecular dynamics calculations, Matsui [111] has also proposed the existence of a new phase at 300 GPa and temperatures above 5000 K. Saxena *et al.* [146] have suggested that α'-iron is the liquidus phase down to a pressure of 60-70 GPa. CM, core-mantle boundary (136 GPa); IOC, inner-outer core boundary (329 GPa); C, center of Earth (364 GPa).

Acknowledgements. Preparation of this compilation was supported by Texas Advanced Research Program Grants 009741-007 and 009741-066, and by National Science Foundation Grants EAR-8816044 and EAR-9219159. Contribution no. 738, Geosciences Program, University of Texas at Dallas.

REFERENCES

1. Ahrens, T. J., H. Tan, and J. D. Bass, Analysis of shock temperature data for iron, *High-Press. Res.*, *2*, 145-157.
2. Akaogi, M., and S. Akimoto, Pyroxene-garnet solid-solution equilibria in the systems $Mg_4Si_4O_{12}$-$Mg_3Al_2Si_3O_{12}$ and $Fe_4Si_4O_{12}$-$Fe_3Al_2Si_3O_{12}$ at high pressures and temperatures, *Phys. Earth and Planet. Int.*, *15*, 90-106, 1977.
3. Akaogi, M., E. Ito, and A. Navrotsky, Olivine-modified spinel-spinel transitions in the system Mg_2SiO_4-Fe_2SiO_4: Calorimetric measurements, thermochemical calculation, and geo-

physical application, *J. Geophys. Res., 94,* 15,671-15,685, 1989.

4. Akaogi, M., and A. Navrotsky, The quartz - coesite - stishovite transformations: New calorimetric measurements and calculation of phase diagrams, *Phys. Earth Planet. Int., 36,* 124-134, 1984.

5. Akella, J., Quartz ↔ coesite transition and the comparative friction measurements in piston-cylinder apparatus using talc-alsimag-glass (TAG) and NaCl high-pressure cells, *Neues Jahrb. Mineral. Monatsh., 5,* 217-224, 1979.

6. Akimoto, S., T. Yagi, T. Suzuki, and O. Shimomura, Phase diagram of iron determined by high pressure X-ray diffraction using synchrotron radiation, in *High Pressure Research in Mineral Physics, Geophys. Monogr. Ser., v. 39,* edited by M. H. Manghnani and Y. Syono, pp. 149-154, Terra Scientific Pub., Tokyo, AGU, Washington, D. C., 1987.

7. Anastasiou, P., and F. Seifert, Solid solubility of Al_2O_3 in enstatite at high temperatures and 1-5 kb water pressure, *Contrib. Mineral. Petrol., 34,* 272-287, 1972.

8. Anderson, O. L., The phase diagram of iron and the temperature of the inner core, *J. Geomag. Geoelec., 45,* 1235-1248, 1993.

9. Atlas, L., The polymorphism of $MgSiO_3$ and solid-state equilibria in the system $MgSiO_3$-$CaMgSi_2O_6$, *J. Geol., 60,* 125-147, 1952.

10. Barth, T. F. W., The feldspar geologic thermometers, *Neues Jahrb. Mineral. Abhandlungen, 82,* 143-154, 1951.

11. Bass, J. D., B. Svendsen, and T. J. Ahrens, The temperature of shock compressed iron, in *High Pressure Research in Mineral Physics, Geophys. Monogr. Ser., v. 39,* edited by M. H. Manghnani and Y. Syono, pp. 393-402, Terra Scientific Pub., Tokyo, AGU, Washington, D. C., 1987.

12. Bell, P. M., and E. H. Roseboom, Jr., Melting relationships of jadeite and albite to 45 kilobars with comments on melting diagrams of binary systems at high pressures, in *Pyroxenes and Amphiboles: Crystal Chemistry and Phase Petrology, Min. Soc. Am. Spec. Paper 2,* edited by J. J. Papike, F. R. Boyd, J. R. Clark, and W. G. Ernst, pp. 151-161, Min. Soc. Am., 1969.

13. Berman, R. G., Internally-consistent thermodynamic data for minerals in the system Na_2O-K_2O-CaO - MgO - FeO - Fe_2O_3 - Al_2O_3-SiO_2-TiO_2-H_2O-CO_2, *J. Petrol, 29,* 445-522, 1988.

14. Biggar, G. M., Calcium-poor pyroxenes: Phase relations in the system CaO-MgO-Al_2O_3-SiO_2, *Min. Mag., 49,* 49-58, 1985.

15. Biggar, G. M., Subsolidus equilibria between protopyroxene, orthopyroxene, pigeonite and diopside, in the $MgSiO_3$-$CaMgSi_2O_6$ at 1 bar to 9.5 kbar, and 1012 to 1450°C, *Eur. J. Mineral., 4,* 153-170, 1992.

16. Birch, F., and P. LeCompte, Temperature-pressure plane for albite composition, *Am. J. Sci., 258,* 209-217, 1960.

17. Boehler, R., The phase diagram of iron to 430 kbar, *Geophys. Res. Lett., 13,* 1153-1156, 1986.

18. Boehler, R., Melting of the Fe-FeO and the Fe-FeS systems at high pressures: Constraints on core temperatures, *Earth Planet. Sci. Lett., 111,* 217-227, 1992.

19. Boehler, R., The phase diagram of iron to 2 Mbar: New static measurements (abstract), *Eos Trans. AGU, 74, No. 16,* 305, 1993.

20. Boehler, R., M. Nicol, and M. L. Johnson, Internally-heated diamond-anvil cell: Phase diagram and P-V-T of iron, in *High Pressure Research in Mineral Physics, Geophys. Monogr. Ser., v. 39,* edited by M. H. Manghnani and Y. Syono, pp. 173-176, Terra Scientific Pub., Tokyo, AGU, Washington, D. C., 1987.

21. Boehler, R., N. von Bargen, and A. Chopelas, Melting, thermal expansion, and phase transitions of iron at high pressures, *J. Geophys. Res., 95,* 21,731-21,736, 1990.

22. Boettcher, A. L., and P. J. Wyllie, Jadeite stability measured in the presence of silicate liquids in the system $NaAlSiO_4$-SiO_2-H_2O, *Geochim. Cosmochim. Acta, 32,* 999-1012, 1968a.

23. Boettcher, A. L., and P. J. Wyllie, The quartz-coesite transition measured in the presence of a silicate liquid and calibration of piston-cylinder apparatus, *Contrib. Mineral. Petrol., 17,* 224-232, 1968b.

24. Bohlen, S. R., and A. L. Boettcher, The quartz ↔ coesite transformation: A precise determination and the effects of other components, *J. Geophys. Res., 87,* 7073-7078, 1982.

25. Boness, D. A., and J. M. Brown, The electronic band structures of iron, sulfur, and oxygen at high pressures and the Earth's core, *J. Geophys. Res., 95,* 21,721-21,730, 1990.

26. Bowen, N. L., The melting phenomena of the plagioclase feldspars, *Am. J. Sci., 35,* 577-599, 1913.

27. Bowen, N. L., and J. F. Schairer, The system MgO-FeO-SiO_2, *Am. J. Sci., 29,* 151-217, 1935.

28. Bowen, N. L., and O. F. Tuttle, The system MgO-SiO_2-H_2O, *Bull. Geol. Soc. Am., 60,* 439-460, 1949.

29. Bowen, N. L., and O. F. Tuttle, The system $NaAlSi_3O_8$-$KAlSi_3O_8$-H_2O, *J. Geol., 58,* 489-511, 1950.

30. Boyd, F. R., Garnet peridotites and the system $CaSiO_3$-$MgSiO_3$-Al_2O_3, in *Fiftieth Anniversary Symposia: Mineralogy and petrology of the upper mantle, sulfides, mineralogy and geochemistry of non-marine evaporites, Min. Soc. America Special Paper 3,* edited by B. A. Morgan, pp. 63-75, Min. Soc. Am., 1970.

31. Boyd, F. R., and J. L. England,

The quartz-coesite transition, *J. Geophys. Res.*, *65*, 749-756, 1960.

32. Boyd, F. R., and J. L. England, Mantle minerals, *Carnegie Inst. Washington Year Book 61*, 107-112, 1962.
33. Boyd, F. R., and J. L. England, Effect of pressure on the melting of diopside, $CaMgSi_2O_6$, and albite, $NaAlSi_3O_8$, in the range up to 50 kilobars, *J. Geophys. Res.*, *68*, 311-323, 1963.
34. Boyd, F. R., and J. L. England, The system enstatite-pyrope, *Carnegie Inst. Wash. Year Book 63*, 157-161, 1964.
35. Boyd, F. R., J. L. England, and B. T. C. Davis, Effects of melting and polymorphism of enstatite, $MgSiO_3$, *J. Geophys. Res.*, *69*, 2101-2109, 1964.
36. Boyd, F. R., and J. F. Schairer, The system $MgSiO_3$-$CaMgSi_2O_6$, *J. Petrol.*, *5*, 275-309, 1964.
37. Brey, G., and J. Huth, The enstatite-diopside solvus to 60 kbar, *Proc. Third Int. Kimberlite Conf.*, *2*, 257-264, 1984.
38. Brown, J. M., and R. G. McQueen, Phase transitions, Grüneisen parameter, and elasticity for shocked iron between 77 GPa and 400 GPa, *J. Geophys. Res.*, *91*, 7485-7494, 1986.
39. Brown, W. L., and I. Parsons, Towards a more practical two-feldspar geothermometer, *Contrib. Mineral Petrol.*, *76*, 369-377, 1981.
40. Bundy, F. P., Pressure-temperature phase diagram of iron to 200 kbar, 900°C, *J. Appl. Phys.*, *36*, 616-620, 1965.
41. Carlson, W. D., Evidence against the stability of orthoenstatite above 1005°C at atmospheric pressure in CaO-MgO-SiO_2, *Geophys. Res. Lett.*, *12*, 490-411, 1985.
42. Carlson, W. D., Reversed pyroxene phase equilibria in CaO-MgO-SiO_2 at one atmosphere pressure, *Contrib. Mineral. Petrol.*, *29*, 218-224, 1986.
43. Carlson, W. D., Subsolidus phase equilibria on the forsterite-saturated join $Mg_2Si_2O_6$-$CaMgSi_2O_6$ at atmospheric pressure, *Am. Mineral.*, *73*, 232-241, 1988.
44. Carlson, W. D., and D. H. Lindsley, Thermochemistry of pyroxenes on the join $Mg_2Si_2O_6$-$CaMgSi_2O_6$, *Am. Mineral.*, *73*, 242-252, 1988.
45. Chen, C.-H., and D. C. Presnall, The system Mg_2SiO_4-SiO_2 at pressures up to 25 kilobars, *Am. Mineral.*, *60*, 398-406, 1975.
46. Darken, L. S., and R. W. Gurry, The system iron-oxygen, I. The wüstite field and related equilibria, *J. Am. Chem. Soc.*, *67*, 1398-1412, 1945.
47. Darken, L. S., and R. W. Gurry, The system iron-oxygen. II. Equilibrium and thermodynamics of liquid oxide and other phases, *J. Am. Chem. Soc.*, *68*, 798-816, 1946.
48. Davis, B. T. C., and J. L. England, The melting of forsterite up to 50 kilobars, *J. Geophys. Res.*, *69*, 1113-1116, 1964.
49. Elkins, L. T., and T. L. Grove, Ternary feldspar experiments and thermodynamic models, *Am. Mineral.*, *75*, 544-559, 1990.
50. Essene, E. J., Geologic thermometry and barometry, in *Characterization of Metamorphism Through Mineral Equilibria, Rev. Min., Min. Soc. Am.*, *10*, edited by J. M. Ferry, 153-206, 1982.
51. Fei, Y., H.-K. Mao, and B. O. Mysen, Experimental determination of element partitioning and calculation of phase relationships in the MgO-FeO-SiO_2 system at high pressure and high temperature, *J. Geophys. Res.*, *96*, 2157-2169, 1991.
52. Foley, S., High-pressure stability of the fluor- and hydroxy-endmembers of pargasite and K-richterite, *Geochim. Cosmochim. Acta*, *55*, 2689-2694, 1991.
53. Fuhrman, M. L., and D. H. Lindsley, Ternary feldspar modeling and thermometry, *Am. Mineral.*, *73*, 201-215, 1988.
54. Gallagher, K. G., and T. J. Ahrens, First measurements of thermal conductivity in griceite and corundum at ultra high pressure and the melting point of iron (abstract), *Eos Trans. AGU*, *75*, *No. 44*, 653, 1994.
55. Gasparik, T., Transformation of enstatite-diopside-jadeite pyroxenes to garnet, *Contrib. Mineral. Petrol.*, *102*, 389-405, 1989.
56. Gasparik, T., A thermodynamic model for the enstatite-diopside join, *Am. Mineral.*, *75*, 1080-1091, 1990a.
57. Gasparik, T., Phase relations in the transition zone, *J. Geophys. Res.*, *95*, 15,751-15,769, 1990b.
58. Ghiorso, M. S., Activity/composition relations in the ternary feldspars, *Contrib. Mineral. Petrol.*, *87*, 282-296, 1984.
59. Gilbert, M. C., Reconnaissance study of the stability of amphiboles at high pressure, *Carnegie Inst. Washington Year Book 67*, 167-170, 1969.
60. Gilbert, M. C., R. T. Helz, R. K. Popp, and F. S. Spear, Experimental studies of amphibole stability, in *Amphiboles: Petrology and Experimental Phase Relations*, edited by D. R. Veblen and P. H. Ribbe, *Rev. Mineralogy, 9B, Chapter 2*, pp. 229-353, 1982.
61. Giles, P. M., M. H. Longenbach, and A. R. Marder, High pressure martensitic transformation in iron, *J. Appl. Phys.*, *42*, 4290-4295, 1971.
62. Green, D. H., A. E. Ringwood, and A. Major, Friction affects and pressure calibration in a piston-cylinder apparatus at high pressure and temperature, *J. Geophys. Res.*, *71*, 3589-3594, 1966.
63. Green, N. L., and S. I. Udansky, Ternary-feldspar mixing relations and feldspar thermobarometry, *Am. Mineral.*, *71*, 1100-1108, 1986.
64. Greig, J. W., E. Posnjak, H. E. Merwin, and R. B. Sosman, Equilibrium relationships of Fe_3O_4, Fe_2O_3, and oxygen, *Am. J. Sci.*, *30*, 239-316, 1935.

65. Grover, J. E., The stability of low-clinoenstatite in the system Mg_2SiO_4 - $CaMgSi_2O_6$ (abstract), *Eos Trans. AGU, 53*, 539, 1972.
66. Haselton, H. T., Jr., G. L. Hovis, B. S. Hemingway, and R. A. Robie, Calorimetric investigation of the excess entropy of mixing in analbite-sanidine solid solutions: Lack of evidence for Na, K short-range order and implications for two-feldspar thermometry, *Am. Mineral., 68*, 398-413, 1983.
67. Hays, J. F., Lime-alumina-silica, *Carnegie Inst. Washington Year Book 65*, 234-239, 1966.
68. Henderson, C. M. B., Graphical analysis of phase equilibria in An-Ab-Or, in *Progress in Experimental Petrology, Nat. Environ. Res. Council Pub. 25, Series D*, edited by C. M. B. Henderson, pp. 70-78, University Press, Cambridge, 1984.
69. Herzberg, C., and T. Gasparik, Garnet and pyroxenes in the mantle: A test of the majorite fractionation hypothesis, *J. Geophys. Res., 96*, 16,263-16,274, 1991.
70. Holland, T. J. B., and R. Powell, An enlarged and updated internally consistent thermodynamic data set with uncertainties and correlations: The system K_2O-Na_2O - CaO - MgO - MnO - FeO-Fe_2O_3-Al_2O_3-TiO_2-SiO_2-C-H_2-O_2, *J. Met. Geol., 8*, 89-124, 1990.
71. Holloway, J. R., The system pargasite-H_2O-CO_2: A model for melting of a hydrous mineral with a mixed volatile fluid - I. Experimental results to 8 kbar, *Geochim. Cosmochim. Acta, 37*, 651-666, 1973.
72. Holloway, J. R., and C. E. Ford, Fluid-absent melting of the fluoro-hydroxy amphibole pargasite to 35 kilobars, *Earth Planet. Sci. Lett., 25*, 44-48, 1975.
73. Huang, E., W. A. Bassett, and P. Tao, Study of bcc-hcp iron phase transition by synchrotron radiation, in *High Pressure Research in Mineral Physics, Geophys. Monogr. Ser., v. 39*, edited by M. H. Manghnani and Y. Syono, pp. 165-172, Terra Scientific Pub., Tokyo, AGU, Washington, D.C., 1987.
74. Huckenholz, H. G., M. C. Gilbert, and T. Kunzmann, Stability and phase relations of calcic amphiboles crystallized from magnesiohastingsite compositions in the 1 to 45 kbar pressure range, *Neues Jahrbuch Miner. Abh., 164*, 229-268, 1992.
75. Iiyama, J. T., Contribution à l'étude des équilibre sub-solidus du système ternaire orthoso-albite-anorthite à l'aide des réactions d'echenge d'ions Na-K au contact d'une solution hydrothermale, *Bull. Soc Minéral. Cryst. Français, 89*, 442-454, 1966.
76. Ito, E., and E. Takahashi, Post-spinel transformations in the system Mg_2SiO_4-Fe_2SiO_4 and some geophysical implications, *J. Geophys. Res., 94*, 10,637-10,646, 1989.
77. Jackson, I., Melting of the silica isotypes SiO_2, BeF_2, and GeO_2 at elevated pressures, *Phys. Earth Planet. Int., 13*, 218-231, 1976.
78. Jenner, G. A., and D. H. Green, Equilibria in the Mg-rich part of the pyroxene quadrilateral, *Min. Mag., 47*, 153-160, 1983.
79. Johannes, W., Melting of plagioclase in the system ab-an-H_2O and qz-ab-H_2O at P_{H_2O} = 5 kbars, an equilibrium problem, *Contrib. Mineral. Petrol. 66*, 295-303, 1978.
80. Johannes, W., Ternary feldspars: Kinetics and possible equilibria at 800°C, *Contrib. Mineral. Petrol., 68*, 221-230, 1979.
81. Johannes, W., D. W. Chipman, J. F. Hays, P. M. Bell, H. K. Mao, R. C. Newton, A. L. Boettcher, and F. Seifert, An interlaboratory comparison of piston-cylinder pressure calibration using the albite-breakdown reaction, *Contrib. Mineral. Petrol., 32*, 24-38, 1971.
82. Kanzaki, M., Ultrahigh-pressure phase relations in the system $Mg_4Si_4O_{12}$-$Mg_3Al_2Si_3O_{12}$, *Phys. Earth Planet. Inter., 49*, 168-175, 1987.
83. Kanzaki, M., Melting of silica up to 7 GPa, *J. Am. Ceram. Soc., 73*, 3706-3707, 1990.
84. Kato, T., and M. Kumazawa, Effect of high pressure on the melting relation in the system Mg_2SiO_4-$MgSiO_3$ Part I. Eutectic relation up to 7 GPa, *J. Phys. Earth, 33*, 513-524, 1985a.
85. Kato, T., and M. Kumazawa, Stability of phase B, a hydrous magnesium silicate, to 2300°C at 20 GPa, *Geophys. Res. Lett., 12*, 534-535, 1985b.
86. Kato, T., and M. Kumazawa, Melting and phase relations in the system Mg_2SiO_4-$MgSiO_3$ at 20 GPa under hydrous conditions, *J. Geophys. Res., 91*, 9351-9355, 1986.
87. Katsura, T., and E. Ito, The system Mg_2SiO_4-Fe_2SiO_4 at high pressures and temperatures: Precise determination of stabilities of olivine, modified spinel, and spinel, *J. Geophys. Res., 94*, 15,663-15,670, 1989.
88. Kinomura, N., S. Kume, and M. Koizumi, Stability of $K_2Si_4O_9$ with wadeite type structure, in *Proc. 4th Inter. Conf. on High Pressure,* edited by J. Osugi, pp. 211-214, Phys. Chem. Soc. Japan, 1975.
89. Kitahara, S., and G. C. Kennedy, The quartz-coesite transition, *J. Geophys. Res., 69*, 5395-5400, 1964.
90. Kitahara, S., S. Takanouchi, and G. C. Kennedy, Phase relations in the system MgO-SiO_2-H_2O at high temperatures and pressures, *Am. J. Sci., 264*, 223-233, 1966.
91. Kushiro, I., Determination of liquidus relations in synthetic silicate systems with electron probe analysis: The system forsterite-diopside-silica at 1 atmosphere, *Am. Mineral., 57*, 1260-1271, 1972.
92. Kushiro, I., H. S. Yoder, Jr., and M. Nishikawa, Effect of water on the melting of enstatite, *Geol.*

Soc. Am. Bull., 79, 1685-1692, 1968.

93. Lindsley, D. H., Melting relations of $KAlSi_3O_8$: Effect of pressures up to 40 kilobars, *Am. Mineral, 51*, 1793-1799, 1966.
94. Lindsley, D. H., Melting relations of plagioclase at high pressures, in *New York State Museum and Science Service Memoir 18*, pp. 39-46, 1968.
95. Lindsley, D. H., Pyroxene thermometry, *Am. Mineral., 68*, 477-493, 1983.
96. Lindsley, D. H., Experimental studies of oxide minerals, in *Oxide Minerals: Petrologic and Magnetic Significance, Rev. Mineralogy, 25, Chapter 3*, edited by D. H. Lindsley, 69-106, 1991.
97. Lindsley, D. H., and D. J. Andersen, a two-pyroxene thermometer, *Proc. Thirteenth Lunar Planet. Sci. Conf., Part 2, J. Geophys. Res., 88, Supplement*, A887-A906, 1983.
98. Lindsley, D. H., and S. A. Dixon, Diopside-enstatite equilibria at 850 to 1400°C, 5 to 35 kbars, *Am. J. Sci., 276*, 1285-1301, 1976.
99. Liu, L.-G., Silicate perovskite from phase transformations of pyrope-garnet at high pressures and temperature, *Geophys. Res. Lett., 1*, 277-280, 1974.
100. Liu, L.-G., First occurrence of the garnet-ilmenite transition in silicates, *Science, 195*, 990-991, 1977.
101. Liu, L. G., High-pressure phase transformations of albite, jadeite, and nepheline, *Earth Planet. Sci. Lett., 37*, 438-444, 1978.
102. Liu, L.-G., The system enstatite-wollastonite at high pressures and temperatures with emphasis on diopside, *Phys. Earth Planet. Int., 19*, P15-P18, 1979.
103. Liu, L.-G., and W. A. Bassett, The melting of iron up to 200 kilobars, *J. Geophys. Res., 80*, 3777-3782, 1975.
104. Liu, L.-G., and W. A. Bassett, *Elements, Oxides, Silicates. High-Pressure Phases with Implications for the Earth's Interior*, 250 pp., Oxford Univ. Press, New York, 1986.
105. Liu, L.-G., W. A. Bassett, and J. Sharry, New high-pressure modifications of GeO_2 and SiO_2, *J. Geophys. Res., 83*, 2301-2305, 1978.
106. Longhi, J., and A. E. Boudreau, The orthoenstatite liquidus field in the system forsterite-diopside-silica at one atmosphere, *Am. Mineral., 65*, 563-573, 1980.
107. Manghnani, M. H., L. C. Ming, and N. Nakagiri, Investigation of the α-Fe to ε-iron phase transition by synchrotron radiation, in High Pressure Research in *Mineral Physics, Geophys. Monogr. Ser., v. 39*, edited by M. H. Manghnani and Y. Syono, pp. 155-164, Terra Scientific Pub., Tokyo, AGU, Washington, D. C., 1987.
108. Mao, H. K., W. A. Bassett, and T. Takahashi, Effects of pressure on crystal structure and lattice parameters of iron up to 300 kbar, *J. Appl. Phys., 38*, 272-276, 1967.
109. Mao, H. K., P. M. Bell, and C. Hadidiacos, Experimental phase relations of iron to 360 kbar, 1400°C, determined in an internally heated diamond-anvil apparatus, in *High Pressure Research in Mineral Physics, Geophys. Monogr. Ser., v. 39*, edited by M. H. Manghnani and Y. Syono, pp. 135-138, 1987.
110. Mao, H. K., T. Yagi, and P. M. Bell, Mineralogy of Earth's deep mantle: Quenching experiments on mineral compositions at high pressure and temperature, *Carnegie Inst. Washington Yearbook 76*, 502-504, 1977.
111. Matsui, M., Computer simulation of the structural and physical properties of iron under ultra-high pressures and high temperatures, *Central Core Earth, 2*, 79-82, 1992.
112. Mirwald, P. W., and G. C. Kennedy, The Curie point and the α-γ transition of iron to 53 kbar - a reexamination, *J. Geophys. Res., 84*, 656-658, 1979.
113. Mirwald, P. W., and H.-J. Massonne, The low-high quartz and quartz-coesite transition to 40 kbar between 600° and 1600°C and some reconnaissance data on the effect of $NaAlO_2$ component on the low quartz-coesite transition, *J. Geophys. Res., 85*, 6983-7990, 1980.
114. Modreski, P. J., and A. L. Boettcher, The stability of phlogopite + enstatite at high pressures: A model for micas in the interior of the Earth, *Am. J. Sci., 272*, 852-869, 1972.
115. Modreski, P. J., and A. L. Boettcher, Phase relationships of phlogopite in the system K_2O-MgO-CaO-Al_2O_3-SiO_2-H_2O to 35 kilobars: A better model for micas in the interior of the Earth, *Am. J. Sci., 273*, 385-414, 1973.
116. Montana, A., and M. Brearley, An appraisal of the stability of phlogopite in the crust and in the mantle, *Am. Mineral., 74*, 1-4, 1989.
117. Morey, G. W., Phase-equilibrium relations of the common rock-forming oxides except water, *U. S. Geol. Survey Prof. Paper 440-L*, L1-L158, 1964.
118. Mori, T., and D. H. Green, Pyroxenes in the system $Mg_2Si_2O_6$-$CaMgSi_2O_6$ at high pressure, *Earth Planet. Sci. Lett., 26*, 277-286, 1975.
119. Morse, S. A., Alkali feldspars with water at 5 kb pressure, *J. Petrol., 11*, 221-251, 1970.
120. Muan, A., and E. F. Osborn, *Phase Equilibria Among Oxides in Steelmaking*, 236 pp., Addison-Wesley, Reading, MA, 1965.
121. Nekvasil, H., and D. H. Lindsley, Termination of the 2 feldspar + liquid curve in the system Ab-Or-An-H_2O at low H_2O contents, *Am. Mineral., 75*, 1071-1079, 1990.
122. Newton, R. C., Thermodynamic analysis of phase equilibria in simple mineral systems, in *Thermodynamic Modeling of Geological Materials: Minerals, Fluids, and Melts, Rev. Mineral.,*

Mineral Soc. Am. 17, edited by I. S. E. Carmichael and H. P. Eugster, pp. 1-33, 1987.

123. Nickel, K. G., and G. Brey, Subsolidus orthopyroxene-clinopyroxene systematics in the system CaO-MgO-SiO_2 to 60 kbar. A reevaluation of the regular solution model, *Contrib. Mineral. Petrol., 87,* 35-42, 1984.
124. Oba, T., Experimental study on the tremolite-pargasite join at variable temperatures under 10 kbar, *Proc. Indian Acad. Sci., 99,* 81-90, 1990.
125. Ohtani, E., T. Irifune, and K. Fujino, Fusion of pyrope at high-pressures and rapid crystal growth from the pyrope melt, *Nature, 294,* 62-64, 1981.
126. Ohtani, E., and M. Kumazawa, Melting of forsterite Mg_2SiO_4 up to 15 GPa, *Phys. Earth Planet. Inter., 27,* 32-38, 1981.
127. Pacalo, R. I. G., and T. Gasparik, Reversals of the orthoenstatite-clinoenstatite transition at high pressures and high temperatures, *J. Geophys. Res., 95,* 15,853-15,858, 1990.
128. Perkins, D., III, and R. C. Newton, The composition of coexisting pyroxenes and garnet in the system CaO-MgO-Al_2O_3-SiO_2 at 900-1100°C and high pressures, *Contrib. Mineral. Petrol., 75,* 291-300, 1980.
129. *Phase Diagrams for Ceramists, Vol. 1,* edited by E. M. Levin, C. R. Robbins, and H. F. McMurdie, 601 pp., Amer. Ceramic Soc., Columbus, Ohio, 1964.
130. *Phase Diagrams for Ceramists, Vol. 2,* edited by E. M. Levin and H. F. McMurdie, 625 pp., Amer. Ceramic Soc., Columbus, Ohio, 1969.
131. *Phase Diagrams for Ceramists, Vol. 3,* edited by E. M. Levin, C. R. Robbins, and H. F. McMurdie, 513 pp., Amer. Ceramic Soc., Columbus, Ohio, 1975.
132. *Phase Diagrams for Ceramists, Vol. 4,* edited by R. S. Roth, T. Negas, and L. P. Cook, 330 pp., Amer. Ceramic Soc., Columbus, Ohio, 1981.
133. *Phase Diagrams for Ceramists, Vol. 5,* edited by R. S. Roth, T. Negas, and L. P. Cook, 395 pp., Amer. Ceramic Soc., Columbus, Ohio, 1983.
134. *Phase Diagrams for Ceramists, Cumulative Index,* 495 pp., Amer. Ceramic Soc., Columbus, Ohio, 1984.
135. *Phase Diagrams for Ceramists, Vol. 6,* edited by R. S. Roth, J. R. Dennis, and H. F. McMurdie, 515 pp., Amer. Ceramic Soc., Columbus, Ohio, 1987.
136. *Phase Diagrams for Ceramists, Vol. 7,* 591 pp., Amer. Ceramic Soc., Columbus, Ohio, 1989.
137. *Phase Diagrams for Ceramists, Vol. 8,* edited by B. O. Mysen, 399 pp., Amer. Ceramic Soc., Columbus, Ohio, 1989.
138. Phillips, B., and A. Muan, Stability relations of iron oxides: phase equilibria in the system Fe_3O_4-Fe_2O_3 at oxygen pressures up to 45 atmospheres, *J. Phys. Chem., 64,* 1451-1453, 1960.
139. Powell, M, and R. Powell, Plagioclase-alkali feldspar geothermometry revisited, *Min. Mag., 41,* 253-256, 1977.
140. Presnall, D. C., and T. Gasparik, Melting of enstatite ($MgSiO_3$) from 10 to 16.5 GPa and the forsterite (Mg_2SiO_4) - majorite ($MgSiO_3$) eutectic at 16.5 GPa: Implications for the origin of the mantle, *J. Geophys. Res., 95,* 15,771-15,777, 1990.
141. Presnall, D. C., and M. J. Walter, Melting of forsterite, Mg_2SiO_4, from 9.7 to 16.5 GPa, *J. Geophys. Res., 98,* 19,777-19,783, 1993.
142. Price, J. G., Ideal site-mixing in solid solutions with applications to two-feldspar geothermometry, *Am. Mineral., 70,* 696-701, 1985.
143. Ringwood, A. E., and W. Hibberson, The system Fe-FeO revisited, *Phys. Chem. Miner. 17,* 313-319, 1990.
144. Ringwood, A. E., A. F. Reid, and A. D. Wadsley, High-pressure $KAlSi_3O_8$, an aluminosilicate with sixfold coordination, *Acta Cryst., 23,* 1093-1095, 1967.
145. Ross, M., D. A. Young, and R. Grover, Theory of the iron phase diagram at Earth core conditions, *J. Geophys. Res., 95,* 21,713-21,716, 1990.
146. Saxena, S. K., G. Shen, and P. Lazor, High pressure phase equilibrium data for iron: Discovery of a new phase with implications for Earth's core, *EOS Trans. Am. Geophys. Union, 74,* 305.
147. Sawamoto, H., Phase diagram of $MgSiO_3$ at pressures up to 24 GPa and temperatures up to 2200°C: Phase stability and properties of tetragonal garnet, in *High Pressure Research in Mineral Physics, Geophys. Monogr. Ser., v. 39,* edited by M. H. Manghnani and Y. Syono, pp. 209-219, Terra Scientific Pub., Tokyo, AGU, Washington, D. C., 1987.
148. Schairer, J. F., The alkali-feldspar join in the system $NaAlSiO_4$-$KAlSiO_4$-SiO_2, *J. Geol., 58,* 512-517, 1950.
149. Schairer, J. F., and N. L. Bowen, The system K_2O-Al_2O_3-SiO_2, *Am. J. Sci., 253,* 681-746, 1955.
150. Schweitzer, E., The reaction pigeonite = diopside$_{ss}$ + enstatite$_{ss}$ at 15 kbars, *Am. Mineral., 67,* 54-58, 1982.
151. Seck, H. A., Die einfluβ des drucks auf die zusammensetzung koexistierende alkalifeldspate und plagioklase im system $NaAlSi_3O_8$-$KAlSi_3O_8$-$CaAl_2Si_2O_8$-H_2O, *Contrib. Mineral. Petrol., 31,* 67-86, 1971a.
152. Seck, H. A., Koexistierende alkalifeldspate und plagioklase im system $NaAlSi_3O_8$-$KAlSi_3O_8$-$CaAl_2Si_2O_8$-H_2O bei temperaturen von 650°C bis 900°C, *Neues Jahrb. Mineral. Abhandlungen, 115,* 315-342, 1971b.
153. Shen, G., P. Lazor, and S. K. Saxena, Laser-heated diamond-anvil cell experiments at high pressures. II. Melting of iron and

wüstite (abstract), *Eos Trans. AGU, 73, No. 14*, 368, 1992.

154. Spear, F. S. and J. T. Chaney, A petrogenetic grid for pelitic schists in the system SiO_2-Al_2O_3-FeO - MgO - K_2O - H_2O, *Contrib. Mineral. Petrol., 101*, 149-164, 1989.
155. Spencer, K. J., and D. H. Lindsley, A solution model for coexisting iron-titanium oxides, *Am. Mineral., 66*, 1189-1201, 1981.
156. Stewart, D. B., and E. H. Roseboom, Jr., Lower temperature terminations of the three-phase region plagioclase-alkali feldspar -liquid, *J. Petrol., 3*, 280-315, 1962.
157. Stixrude, L., and M. S. T. Bukowinski, Stability of (Mg,Fe)SiO_3 perovskite and the structure of the lowermost mantle, *Geophys. Res. Lett., 19*, 1057-1060, 1992.
158. Stormer, J. C., Jr., A practical two-feldspar geothermometer, *Am. Mineral., 60*, 667-674, 1975.
159. Strong, H. M., R. E. Tuft, and R. E. Hannemann, The iron fusion curve and the triple point, *Metall. Trans., 4*, 2657-2611, 1973.
160. Suito, K., Phase relations of pure Mg_2SiO_4 up to 200 kilobars, in *High-Pressure Research,* edited by M. H. Manghnani and S. Akimoto, pp. 255-266, Academic Press, 1977.
161. Taylor, R. W., Phase equilibria in the system FeO-Fe_2O_3-TiO_2 at 1300°C, *Am. Mineral., 49,* 1016-1030, 1964.
162. Togaya, M., High pressure generation and phase transformations of SiO_2 and GeO_2, in *High Pressure in Science and Technology*, *Mat. Res. Symp. Proc., 22*, edited by C. Homan, R. K. MacCrone, and E. Whalley, 373-376, 1984.
163. Tsuchida, Y., and T. Yagi, A new post-stishovite high-pressure polymorph of silica, *Nature, 340,* 217-220, 1989.
164. Tuttle, O. F., and N. L. Bowen, Origin of granite in the light of experimental studies in the system $NaAlSi_3O_8$-$KAlSi_3O_8$-SiO_2-H_2O, *Geol Soc. Am. Mem. 74,* 153 pp., 1958.
165. Whitney, J. A., and J. C. Stormer, Jr., The distribution of $NaAlSi_3O_8$ between coexisting microcline and plagioclase and its effect on geothermometric calculations, *Am. Mineral, 62*, 687-691, 1977.
166. Williams, D. W., and Kennedy, G. C., Melting curve of diopside to 50 kilobars, *J. Geophys. Res., 74*, 4359-5366, 1969.
167. Williams, Q., R. Jeanloz, J. Bass, B. Svendsen, and T. J. Ahrens, The melting curve of iron to 250 gigapascals: A constraint on the temperature at Earth's core, *Science, 236*, 181-183, 1987.
168. Yagi, T., and S. Akimoto, Direct determination of coesite-stishovite transition by in-situ X-ray measurements, *Tectonophys., 35*, 259-270, 1976.
169. Yamamoto, K., and S. Akimoto, The system MgO-SiO_2-H_2O at high pressures and temperatures - Stability field for hydroxyl-chondrodite, hydroxy-clinohumite and 10 Å-phase, *Am. J. Sci., 277,* 288-312, 1977.
170. Yang, H.-Y., Crystallization of iron-free pigeonite in the system anorthite-diopside-enstatite-silica at atmospheric pressure, *Am. J. Sci., 273*, 488-497, 1973.
171. Yang, H.-Y., and W. R. Foster, Stability of iron-free pigeonite at atmospheric pressure, *Am. Mineral., 57*, 1232-1241, 1972.
172. Yoder, H. S., Jr., High-low quartz inversion up to 10,000 bars, *Trans. AGU, 31*, 827-835, 1950.
173. Yoder, H. S., Jr., Change of melting point of diopside with pressure, *J. Geol., 60*, 364-374, 1952.
174. Yoder, H. S., Jr., and I. Kushiro, Melting of a hydrous phase: phlogopite, *Am. J. Sci., 267-A*, 558-582, 1969.
175. Yoder, H. S., Jr., D. B. Stewart, and J. R. Smith, Ternary feldspars, *Carnegie Inst. Washington Year Book 56*, 206-214, 1957.
176. Yoo, C. S., N. C. Holmes, M. Ross, D. J. Webb, and C. Pike, Shock temperatures and melting of iron at Earth core conditions, *Phys. Rev. Lett., 70*, 3931-3934, 1993.
177. Zerr, A., and Boehler, R., Melting of (Mg,Fe)SiO_3-perovskite under hydrostatic, inert conditions to 580 kbar (abstract), *Eos Trans. AGU, 74, No. 16*, 168-169, 1993.
178. Zhang, J., R. C. Liebermann, T. Gasparik, C. T. Herzberg, and Y. Fei, Melting and subsolidus relations of SiO_2 at 9-14 GPa, *J. Geophys. Res., 98,* 19,785-19,793, 1993.
179. Zou, G., P. M. Bell, and H. K. Mao, Application of the solid-helium pressure medium in a study of the α-ε Fe transition under hydrostatic pressure, *Carnegie Inst. Washington Year Book 80*, 272-274, 1981.